IOCU 2026 Conference

The 3rd International Online Conference on Universe

4–6 March 2026 | Online

MDPI

An analysis of triply ionized carbon absorption in the spectrum of Q1422+23

Satyajit Pal*

satyajitpal1995@gmail.com

Department of Mathematics, Dr. Bhupendra Nath Dutta Smriti Mahavidyalaya, Hatgobindapur, Purba Bardhaman, West Bengal, India -713407

Introduction

High redshift quasars serve as exceptionally luminous background beacons that illuminate the diffuse and structured gas distributed along the line of sight. As the quasar radiation traverses intervening regions, distinct absorption features are imprinted carries information about their kinematics, ionization conditions and chemical composition. Among these diagnostics, the C IV resonance doublet at 1548.204 Å and 1550.774 Å is a particularly powerful tracer of highly ionized, metal enriched gas associated with the intergalactic medium and the circumgalactic environments of forming galaxies. The high emission redshift of Q1422+23 (z_{em} ≈ 3.62) places it at a cosmological epoch when early star formation and feedback processes were actively enriching the universe.

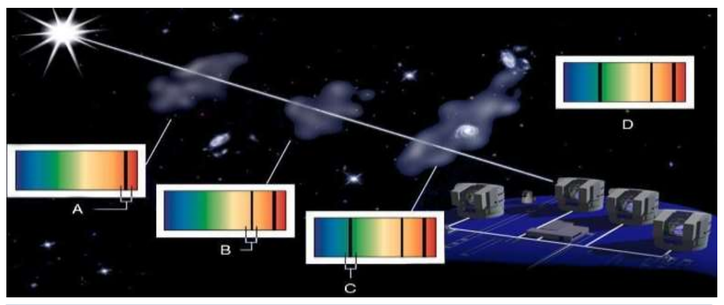

Objectives

Using the quasar Q1422+23 (z_{em} = 3.620), this work aims to identify C IV absorption systems along the line of sight through the characteristic λλ1548, 1550 doublet signature. High spectral resolution (R ≈ 45,000) and excellent signal-to-noise ratio (SNR ≈ 217), provides a sensitive probe of ionized metal-enriched gas at early cosmic epochs. Voigt profile fitted to derive the absorber redshift (z_{abs}), Doppler parameter (b), column density (N_{CIV}) and internal velocity structure. These measurements enable a quantitative assessment of the kinematic and physical properties of the ionised gas and provide insight into the distribution and enrichment of highly ionised carbon in the high redshift universe.

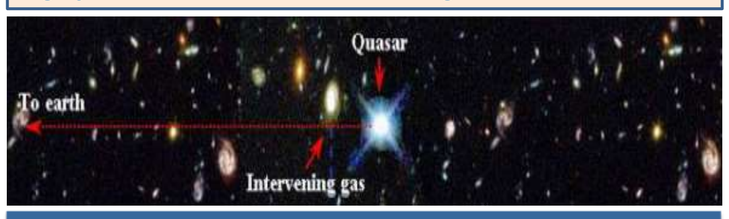

Voigt Profile : Convolution of Gaussian and Lorentzian profile

Gaussian Profile

$$G(\nu) = \frac{1}{\sigma\sqrt{2\pi}} \exp\left[-\frac{(\nu-\nu_0)^2}{2\sigma^2}\right]$$ Where $\sigma = \Delta\nu_D/\sqrt{2}$, $\Delta\nu_D = \frac{\nu_0}{c}\sqrt{\frac{2kT}{m}}$, $b = \sqrt{\frac{2kT}{m} + v_{\text{turb}}^2}$

Lorentzian Profile

$$L(\nu) = \frac{1}{\pi}\frac{\gamma}{(\nu-\nu_0)^2+\gamma^2}$$

where

- γ is the damping constant

Then the Voigt profile can be written as

$$V(\nu) = \frac{1}{\Delta\nu_D\sqrt{\pi}} H(a,x),$$

where $H(a,x)$

$$H(a,x) = \frac{a}{\pi}\int_{-\infty}^{\infty} \frac{e^{-y^2}}{(x-y)^2+a^2}\,dy.$$

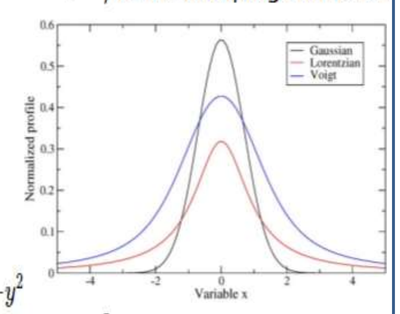

Methodology and Data

Raw Spectrum

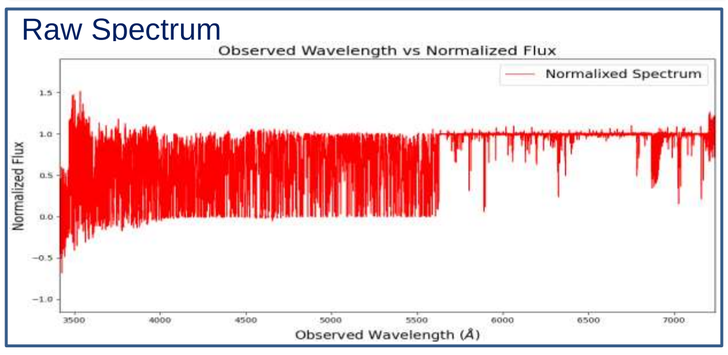

Some CIV absorption lines

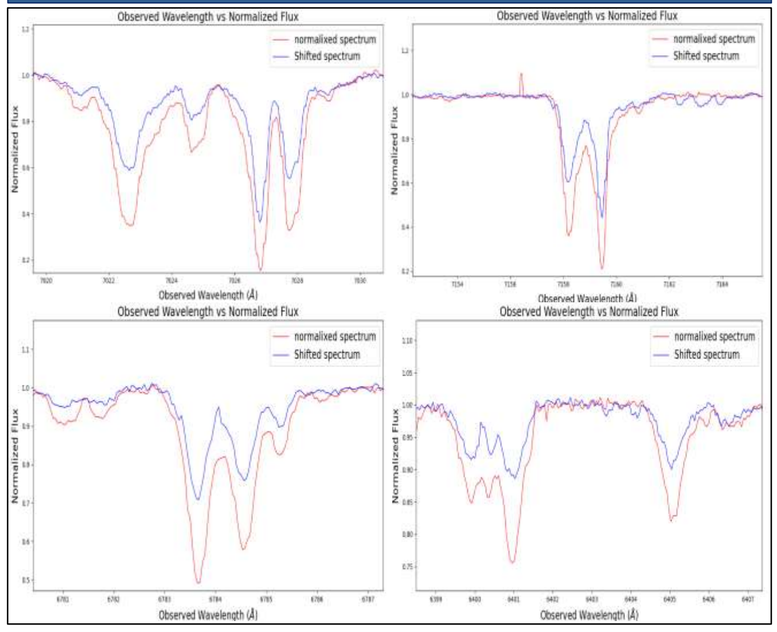

Velocity profiles

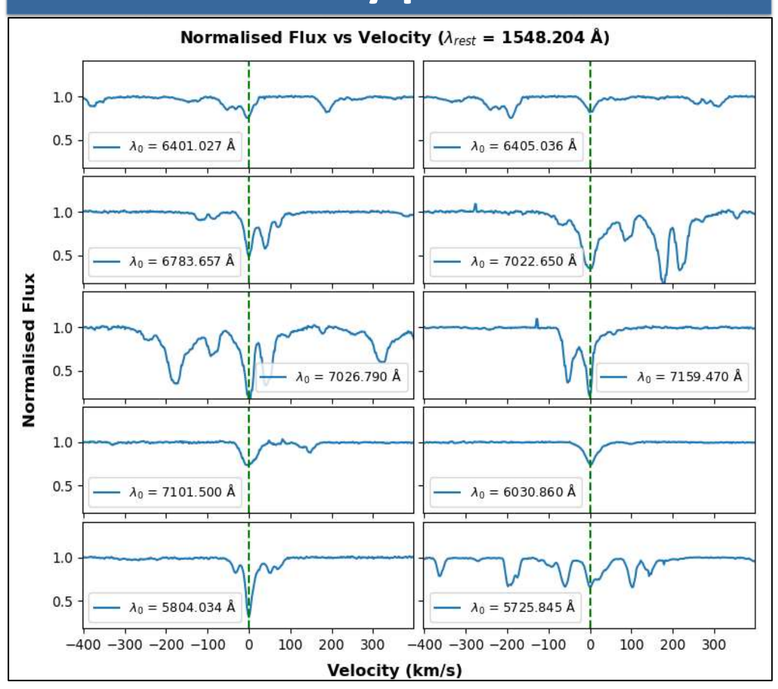

Voigt profile fit

C IV	3.5869415073	0.0000959833	23.03073	8.72144	13.212488	0.144328
C IV	2.8954202139	0.0000646076	21.48341	6.92722	13.120858	0.119930

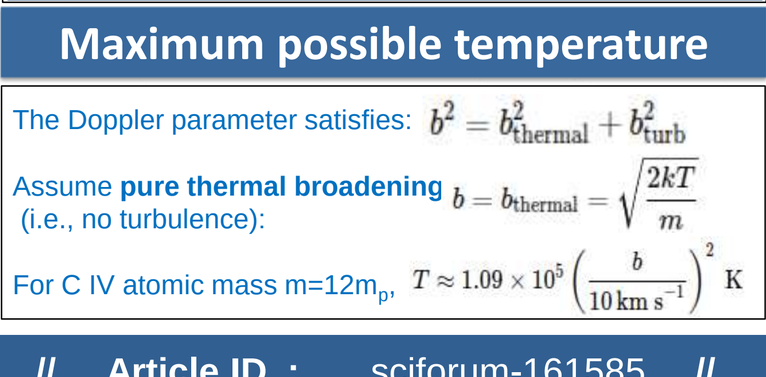

CIV sensitivity and redshift coverage

The Q1422+23 spectrum provides the highest sensitivity in the survey, reaching a limiting detection threshold of

$$\log_{10} N(\mathrm{C\,IV}) = 11.2\ \mathrm{cm}^{-2}$$

This enables detection of very weak, low-column-density absorbers. The absorption analysis covers

$$2.9 \le z \le 3.574,$$

excluding the 3000 km s^{-1} proximity zone, ensuring a clean sample of intervening C IV systems.

Maximum possible temperature

The Doppler parameter satisfies: $b^2 = b_{\text{thermal}}^2 + b_{\text{turb}}^2$

Assume **pure thermal broadening** (i.e., no turbulence): $b = b_{\text{thermal}} = \sqrt{\frac{2kT}{m}}$

For C IV atomic mass m=12m_p, $T \approx 1.09 \times 10^5 \left(\frac{b}{10\,\mathrm{km\,s^{-1}}}\right)^2$ K

z	b	logN	z	b	logN	z	b	logN
2.8954	8.901	12.463	3.089864	13.34	12.943	3.379929	15.299	12.571
2.910039	10.906	11.954	3.090172	20.029	13.173	3.380415	11.914	12.368
2.94722	6.561	11.448	3.090527	20.172	12.989	3.381336	7.432	12.033
2.947508	7.726	12.484	3.091045	10.668	13.006	3.38164	11.618	13.276
2.960624	14.631	12.551	3.094656	17.259	12.225	3.382205	14.003	13.237
2.961076	13.718	12.703	3.119292	13.303	11.91	3.382678	8.59	12.623
2.961436	8.099	12.633	3.119694	12.004	12.047	3.383172	21.22	12.16
2.961945	19.188	13.282	3.13709	13.018	12.608	3.410791	12.722	12.253
2.962325	11.037	12.836	3.137135	29.047	12.615	3.411455	17.96	12.803
2.971356	20.108	12.596	3.13807	20.635	12.268	3.446897	9.693	13.011
2.971625	6.549	11.432	3.191403	8.507	12.127	3.447345	12.356	13.41
2.975182	7.019	11.659	3.233294	8.302	12.035	3.470021	5.055	12.523
2.9758	24.074	12.388	3.242572	3.669	11.528	3.47142	3.327	11.835
2.976199	10.255	12.812	3.256776	14.59	12.049	3.476151	8.083	12.082
2.999203	18.782	12.706	3.257535	22.375	12.3	3.479392	13.929	12.457
3.035023	8.305	12.12	3.265398	9.948	12.063	3.479799	14.623	12.402
3.036582	15.224	12.178	3.265745	17.68	12.599	3.480498	13.49	12.424
3.036909	8.182	11.781	3.275939	11.466	11.893	3.494848	9.965	12.418
3.063372	26.226	12.981	3.317961	13.788	12.186	3.514619	7.946	12.834
3.064317	12.28	12.648	3.535968	23.189	13.733	3.514947	13.446	12.512
3.069583	9.259	12.094	3.536659	22.058	13.053	3.534984	18.519	12.885
3.070155	2.834	11.734	3.537348	19.093	13.245	3.53846	26.345	13.347
3.070996	5.287	12.243	3.538698	9.563	13.585	3.539307	12.178	13.364
3.089864	13.34	12.943	3.539428	17.248	13.231	3.58694	37.908	12.944

The CIV absorbers toward Q1422+23 span a broad range in column density and Doppler parameter, indicating a multi-phase, metal-enriched medium that includes diffuse intergalactic gas and dynamically complex circumgalactic structures shaped by early feedback processes.

z	b	T(K)	Strength	z	b	T(K)	Strength	z	b	T(K)	Strength
2.909662	8.901	8.6×10^4	Moderate	3.070996	5.287	3.0×10^4	Moderate	3.38164	11.618	1.4×10^5	Strong
2.910039	10.906	1.3×10^5	Weak	3.089864	13.34	1.9×10^5	Moderate	3.382205	14.003	2.1×10^5	Strong
2.94722	6.561	4.7×10^4	Weak	3.090172	20.029	4.4×10^5	Strong	3.382678	8.59	8.1×10^4	Moderate
2.947508	7.726	6.5×10^4	Moderate	3.090527	20.172	4.4×10^5	Moderate	3.383172	21.22	4.9×10^5	Moderate
2.960624	14.631	2.3×10^5	Moderate	3.091045	10.668	1.2×10^5	Strong	3.410791	12.722	1.8×10^5	Moderate
2.961076	13.718	2.0×10^5	Moderate	3.094656	17.259	3.2×10^5	Moderate	3.411455	17.96	3.5×10^5	Moderate
2.961436	8.099	7.2×10^4	Moderate	3.119292	13.303	1.9×10^5	Weak	3.446897	9.693	1.0×10^5	Strong
2.961945	19.188	4.0×10^5	Strong	3.119694	12.004	1.6×10^5	Moderate	3.447345	12.356	1.7×10^5	Strong
2.962325	11.037	1.3×10^5	Moderate	3.13709	13.018	1.8×10^5	Moderate	3.470021	5.055	2.8×10^4	Moderate
2.971356	20.108	4.4×10^5	Moderate	3.137135	29.047	9.2×10^5	Moderate	3.47142	3.327	1.2×10^4	Weak
2.971625	6.549	4.7×10^4	Weak	3.13807	20.635	4.6×10^5	Moderate	3.476151	8.083	7.1×10^4	Moderate
2.975182	7.019	5.4×10^4	Weak	3.191403	8.507	8.0×10^4	Moderate	3.479392	13.929	2.1×10^5	Moderate
2.9758	24.074	6.3×10^5	Moderate	3.233294	8.302	7.5×10^4	Moderate	3.479799	14.623	2.3×10^5	Moderate
2.976199	10.255	1.1×10^5	Moderate	3.242572	3.669	1.5×10^4	Weak	3.480498	13.49	2.0×10^5	Moderate
2.999203	18.782	3.8×10^5	Moderate	3.256776	14.59	2.3×10^5	Moderate	3.494848	9.965	1.1×10^5	Moderate
3.035023	8.305	7.5×10^4	Moderate	3.257535	22.375	5.5×10^5	Moderate	3.514619	7.946	6.9×10^4	Moderate
3.036582	15.224	2.5×10^5	Moderate	3.265398	9.948	1.1×10^5	Moderate	3.514947	13.446	2.0×10^5	Moderate
3.036909	8.182	7.3×10^4	Weak	3.265745	17.68	3.4×10^5	Moderate	3.534984	18.519	3.7×10^5	Moderate
3.063372	26.226	7.5×10^5	Moderate	3.275939	11.466	1.4×10^5	Weak	3.535968	23.189	5.8×10^5	Strong
3.064317	12.28	1.6×10^5	Moderate	3.317961	13.788	2.1×10^5	Moderate	3.536659	22.058	5.3×10^5	Strong

- Narrow absorbers → cool photoionized gas $T \approx 2.7 \times 10^4$ K
- Moderate absorbers → mixed thermal + turbulent broadening $T \approx 2.5 \times 10^5$ K
- Broad absorbers → kinematically complex structures $T \approx 1.5 \times 10^6$ K

Discussion and conclusions

- ❖ High–resolution Voigt profile analysis provides a clean and statistically robust characterization of intervening C IV systems across a well-defined redshift interval, ensuring reliable measurements of absorber kinematics and ionic content.
- ❖ The simultaneous presence of narrow, cool absorbers and broader, dynamically complex systems offers direct observational evidence for early feedback-driven metal transport into circumgalactic environments.
- ❖ By quantifying the distribution and physical state of ionized carbon at z = 3.6, this study places meaningful constraints on the timing, efficiency, and large-scale impact of early cosmic metal enrichment.

Future aspects

- ❖ Apply detailed photoionization modelling to constrain metallicity, density, and ionization conditions of the absorbers.
- ❖ Incorporate multi-ion analysis to probe the full multi-phase structure and separate thermal and turbulent contributions.
- ❖ Extend the study to larger quasar samples and compare with simulations to better understand metal enrichment and feedback at high redshift.

References

- Steidel C. C., et al., 2010, ApJ, 717, 289
- Tumlinson J., Peeples M. S., Werk J. K., 2017, ARA&A, 55, 389
- Songaila A., 2001, ApJ, 561, L153
- Becker G. D., Rauch M., Sargent W. L. W., 2009, ApJ, 698, 1010
- Boksenberg A., Sargent W. L. W., 2015, ApJS, 218, 7
- Schaye J., Aguirre A., Kim T.-S., Theuns T., Rauch M., Sargent W. L. W., 2003, ApJ, 596, 768
- Pettini M., Boksenberg A., Hunstead R. W., 1983, ApJ, 273, 436
- Rauch M., 1998, ARA&A, 36, 267
- Simcoe R. A., Sargent W. L. W., Rauch M., 2004, ApJ, 606, 92
- Oppenheimer B. D., Davé R., 2006, MNRAS, 373, 1265